Customizable Coherent Servo Demodulation for Disk Drives

Daniel Y. Abramovitch
Hewlett-Packard Laboratories
Storage Technologies Department
1501 Page Mill Road, M/S 4U-12
Palo Alto, CA 94304 USA
Phone: (650) 857-3806
E-mail: danny@hpl.hp.com

Abstract

This paper describes the Customizable Coherent Demodulation Algorithm, a servo demodulator which provides dramatically improved performance over the currently used servo demodulation methods for disk drives. The demodulation algorithm proposed here makes better use of knowledge about the readback signal coming from the disk to provide better noise immunity and more immunity to other nonidealities in the magnetic head response. The net result is a demodulated Position Error Signal (PES) which has a much cleaner response.

1 Introduction

This paper describes the Customizable Coherent Demodulation Algorithm, an algorithm for servo demodulation in a disk drive that can significantly lower the Position Sensing Noise (PSN)[1] that gets into the servo channel of a disk drive. It does this by mixing the servo burst signal with an idealized version of the dibit response and integrating over a finite, integral number of periods of the waveform. The algorithm differs from demodulation schemes which use rectifiers (in almost all disk drives). It is also different from the amplitude modulated (AM) signal demodulation problem found in communications systems. Typically, the latter are trying to extract a continuous signal rather than a burst of information that yields a single number (as in the case of a servo demodulator). The new algorithm also differs from a Matched Filter demodulator because it allows potentially undesirable portions of the "noise-free signal" to be excluded from the demodulation process.

The main idea is to use the frequency selectivity of an algorithm similar to that used in measuring frequency responses (the swept-sine demodulation algorithm[2]) to achieve far better noise immunity than standard disk drive servo demodulators. A logical question to ask is, "Why has this not been done by others?" The reasons are most likely that:

- such an algorithm is difficult to implement in analog hardware, and
- there has not been a perceived need for such noise immunity in the disk drive servo problem in the past.

However, recent results obtained using the PES Pareto Method[3, 4, 5, 1] have shown that as disk drive servo bandwidths are pushed higher and higher, the amplification by the servo loop of Position Sensing Noise causes major problems. Thus, any method that can reduce the Position Sensing Noise *before* it gets into the servo loop should be quite helpful in allowing the designer to increase the servo bandwidth. Furthermore, the same level of digital hardware that is currently used in modern PRML recording channels should be more than adequate to implement this scheme in real time.

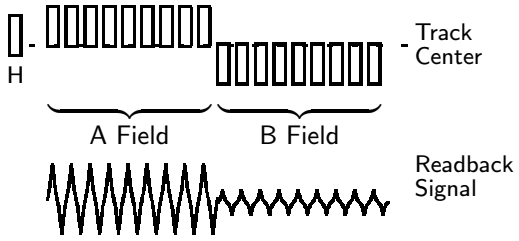

Figure 1: Burst patterns and the resulting readback signals when head is to the left of track center. The magnetic readback head is denoted by the rectangle with the H below. Note that the readback signal is multiplexed in time so that the signal obtained from the A Field is processed separately from the signal obtained from the B Field.

The process of creating a position error signal from amplitude encoded signals on a disk drive may be described as follows. Patterns of alternating magnetic polarity are written on the disk surface with a particular frequency. When the magnetic readback head passes over the burst

pattern, it reads back a signal that is (ideally) periodic for the length of the burst. Nominally, the amplitude of that signal is proportional to how much of the read head is directly over the burst pattern at the time the signal is produced.

To compose a Position Error Signal (PES), two patterns, offset by one track width in the radial direction of the disk and put down sequentially in the down track direction of the disk, are used (Fig. 1). By offsetting these signals, the difference between the amplitude demodulated from the first field (A) and the second field (B), can yield a measure of the radial position of the readback head relative to the disk. Typical disk drives today may have servo patterns on the disk which include 2, 4 or even 6 bursts of position information for a given track. For simplicity of explanation, this paper will discuss only the 2 burst pattern. However, the algorithm applies equally well to all of these cases.

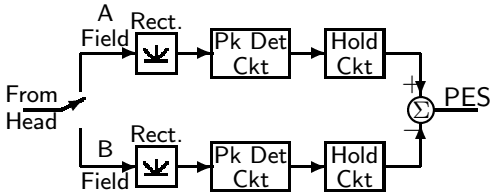

Figure 2: Peak Detection Servo Demodulator

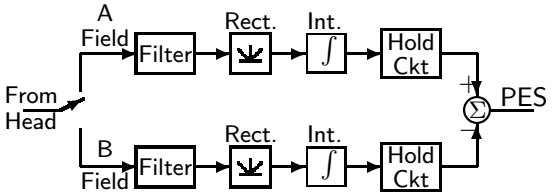

Figure 3: A Rectify and Integrate Servo Demodulator

In a typical disk drive, the servo demodulation is done non-coherently. That is, a nonlinear element is used to produce appropriate harmonics of the signal – rather than mixing the readback signal with a signal which is coherent with the carrier. The signal from the head is passed through a full wave rectifier which computes the absolute value of a signal. The rectifier produces a signal with a large baseband component. For the vast majority of disk drive servo channels, the rectified signal is processed in one of two ways. The first method is Peak (or Envelope) Detection (Fig. 2), in which a circuit is used which detects and holds the peak amplitude value of the rectified signal. The other common method is to integrate the rectified signal (often called Area Detection). Filtering may be added to improve the noise immunity of the Area Detection demodulator (Fig. 3). If done over the right time period, the integration causes all the Fourier components to be averaged to zero except for the baseband term. Broadband noise however, once passed through the rectifier will have a bias, and thus will not average to zero.

The choice between Peak Detection and Area Detection is typically based on the types of distortion that the servo designer expects to encounter. Peak Detection typically results in a simpler circuit design, and it is less prone to certain signal problems (see Section 3.2). On the other hand, integration is essentially an averaging operation, so Area Detection will typically have greater noise immunity than Peak Detection. Because Area Detection uses more sophisticated circuitry than Peak Detection, Area Detection demodulators are often on separate chips from the read channel (see [6], pages 6:21-6:22). Area Detectors are still susceptible to other types of disturbances (see Section 3.2). To deal with some of these issues, manufacturers of these demodulators have begun making hybrid demodulators that contain features from both types of detectors. However, these are still fundamentally non-coherent detectors.

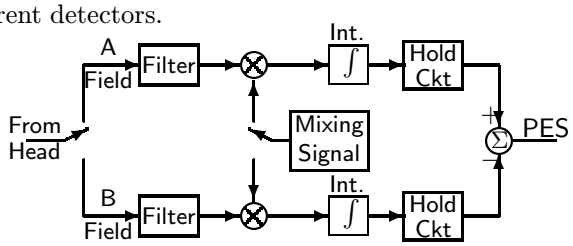

Figure 4: Coherent Servo Demodulation with Optional Filtering

A general block diagram for a coherent demodulator that includes the possibility of pre-filtering the signals is shown in Figure 4. While these diagrams seem pretty straightforward, coherent servo demodulation for disk drives has been attempted in only a few cases. Boutaghou et. al. [7] describe a phase encoded position sensing system. In their demodulator the modulated signal is digitized and then mixed with sine and cosine signals separately. Each of these is summed (in a digital approximation to integration), and the ratio of the sums is computed. Finally, the arctangent of the ratio gives the phase encoded position error signal[7]. Another all-digital coherent demodulation scheme is proposed by Yada and Takeda [8]. They apply a Maximum Likelihood scheme [9] which mixes the sampled modulated signal with a sampled version of the nominal noise-free pulse shape and is considered the optimal solution for rejecting additive white Gaussian noise (AWGN). This method makes use of all the harmonics present in the ideal signal, not simply the first one. It is also worth noting that coherent demodulation has been used in communications system for years.

2 Description of the Algorithm

The method proposed below has several improvements over the aforementioned ones. Like the work by Yada and Takeda [8] and by Boutaghou et. al. [7], it uses a mixing signal that is composed only of a weighted sum of the harmonics of the dibit carrier frequency to achieve improved filtering of broadband noise. Unlike those methods, this algorithm may be implemented in analog, digital, or hybrid forms, while still maintaining the same essential algorithm. Also, unlike those algorithms, the specific harmonics used in the mixing signal can be adjusted to optimize the immunity to both AWGN and nonlinear effects such as the pulse asymmetry from a magneto-resistive (MR) head.

Any of the above methods can be examined in the frequency domain. The ideal dibit pattern (no noise or distortion) produces a periodic signal multiplied by a windowing operation. One can analyze the periodic function using Fourier series analysis [10].

The core idea of this new method can now be described succinctly: *The demodulating signal that is mixed with the dibit signal is composed of a customizable set of harmonics of the noise-free dibit signal.*

By being able to choose *which* harmonics to use, we can optimize the practical performance of the system in the presence of a wide variety of nonidealities (signal distortions) which will be discussed below.

Furthermore, we will discuss implementation strategies which make it easy for the designer to add or remove harmonics at will.

Consider the readback signal from a single burst field with no noise or distortions such as the A Field or the B Field in Figure 1. This signal will begin at a zero value, repeat at each new dibit, and terminate at a zero value. The inverse of the period of a dibit, T, will be the fundamental frequency at which the signal repeats, $f = \frac{1}{T} = \frac{\omega}{2\pi}$. In general, there are M periods of the signal (M dibits) in the burst. We can represent the burst as a product of a periodic signal and a window function. Thus, we can analyze the burst by first analyzing the periodic function.

In general, a periodic signal, $r(t)$, can be analyzed using Fourier series analysis. Due to the symmetry properties of this particular signal and the fact that our signal has a zero DC value and is an odd function, the calculation can be reduced to

$$r(t) = \sum_{n=1}^{\infty} B_n \sin(n\omega t), \ n \text{ odd}. \tag{1}$$

We first consider the signal $r(t) = R_0 \sin\omega t + n(t)$ where $n(t)$ is additive white Gaussian noise (AWGN). We multiply this by the mixing signal, $m(t) = \sin\omega t$. We now integrate this mixed signal for an integral number of periods of the signal, *i.e.,* if $T = \frac{1}{f}$ is the dibit period where $f = \frac{\omega}{2\pi}$, then

$$\frac{1}{MT}\int_0^{MT} m(t)r(t)dt = \frac{R_0}{MT}\int_0^{MT} (\sin\omega t)^2 dt + \frac{1}{MT}\int_0^{MT} (\sin\omega t)n(t)dt. \tag{2}$$

We now use a trigonometric identity and the fact that a sinusoid which is integrated over an integral number of periods integrates to zero. Furthermore, if T is the period of a signal of frequency ω, then it is k periods of a signal of frequency $k\omega$. Combining all of these we get

$$\frac{1}{MT}\int_0^{MT} m(t)r(t)dt = \frac{R_0}{2} + \frac{1}{MT}\int_0^{MT} (\sin\omega t)n(t)dt. \tag{3}$$

Since $n(t)$ is a random variable, we cannot integrate the second term directly. However, we can take the expected value. If we assume that $n(t)$ is a zero mean additive white Gaussian noise, then the expected value of the second term on the right hand side of Equation 2 is 0, leaving the mean dibit amplitude integral, $\overline{R(t)}$, as

$$\overline{R(t)} = E\left\{\frac{1}{MT}\int_0^{MT} m(t)r(t)dt\right\} = \frac{R_0}{2}. \tag{4}$$

Thus, this mixing signal and integration scheme demodulates the amplitude of the signal. Now let us consider the more generalized case of a signal

$$r(t) = R_0\left(r_1 \sin\omega t + r_3 \sin 3\omega t + r_5 \sin 5\omega t\right) + n(t) \tag{5}$$

and the mixing signal $m_1(t) = \sin\omega t$ which yields, through similar operations, $\overline{R(t)} = R_0 r_1/2$. Likewise, we can demodulate the coefficient of the third harmonic by picking $m_3(t) = \sin 3\omega t$, yielding $\overline{R(t)} = R_0 r_3/2$, and the fifth harmonic using $m_5(t) = \sin 5\omega t$, yielding $\overline{R(t)} = R_0 r_5/2$.

2.1 Useful Notes

It should be apparent from this that we can choose to demodulate or ignore *any* individual harmonic. Furthermore, we can compose a single *custom mixing signal* that contains the harmonics that we wish to demodulate and ignores those that we wish to ignore. In particular – unlike the Matched Filter approach – we can choose to ignore some harmonics which may contain distortions peculiar to certain classes of disk drives, but we are free to demodulate any harmonics of the signal that increase our signal to noise ratio. This is an extremely useful property in demodulating disk drive servo position from bursts written on the disk.

Two examples are illustrative here. In the first case we consider $r(t)$ as defined in Equation 5. In this case, choosing

$$m(t) = r_1 \sin\omega t + r_3 \sin 3\omega t + r_5 \sin 5\omega t \tag{6}$$

should maximize the signal to noise ratio. It is equivalent to using a Matched Filter.

The second example comes from the use of Magneto-Resistive (MR) readback heads as the signal transducer. It is often the case that the readback signal is biased on a response curve that behaves nonlinearly with the amplitude of the input signal from the burst. Because of the shape of this curve, the distortion is primarily a quadratic term which adds zeroth and second harmonics to the readback signal:

$$\begin{aligned} r(t) &= R_0 \left(r_1 \sin \omega t + r_3 \sin 3\omega t + r_5 \sin 5\omega t \right. \\ &\quad \left. + k_0 - k_0 \cos 2\omega t\right) + n(t). \end{aligned} \tag{7}$$

The Matched Filter equivalent for this signal involves a mixing signal

$$\begin{aligned} m(t) &= r_1 \sin \omega t + + r_3 \sin 3\omega t + r_5 \sin 5\omega t \\ &\quad + k_1 - k_1 \cos 2\omega t \end{aligned} \tag{8}$$

which maximizes the demodulated signal with respect to the additive white Gaussian noise, $n(t)$, when $k_0 = k_1$. However, this would also demodulate the terms caused by the nonlinear distortion, which may result in a less useful signal for position sensing. In particular, any change in the real time value of k_0 (as might happen with changing track position or MR head bias current) would result in a large error. On the other hand, using the mixing signal defined in Equation 6 would completely avoid the terms which behave nonlinearly with track position. This is the type of flexibility that the algorithm gives us in building a servo demodulator.

It should be noted that if the readback signal takes a different shape, then a sum of cosine waves may also be used in the mixing signal. Furthermore, if synchronization becomes an issue, we can mix with sine and cosine components separately and extract the amplitude and phase of the burst signal.

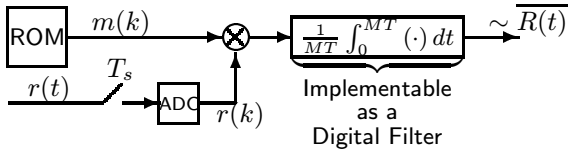

Figure 5: Digital circuit implementation of demodulator.

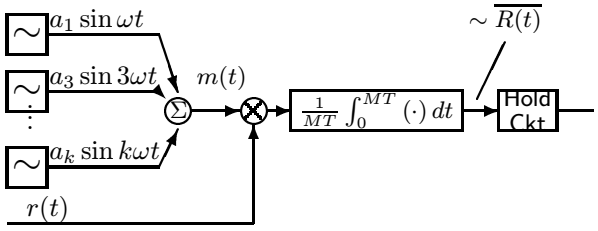

Figure 6: Analog circuit implementation of demodulator.

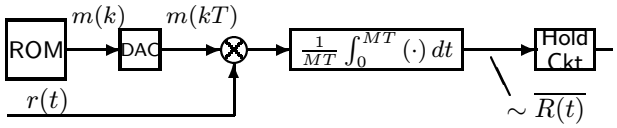

Figure 7: Hybrid analog/digital circuit implementation of demodulator.

Depending upon the hardware available, the new algorithm can be implemented as a fully digital (Figure 5), fully analog (Figure 6), or hybrid implementation (Figure 7).

3 Experimental Results

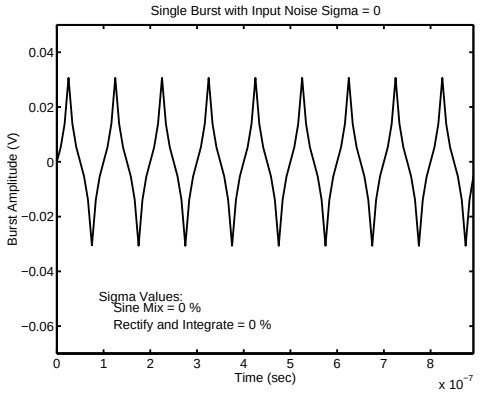

Figure 8: Ideal burst signal with no noise and no nonidealities.

The new algorithm has been successfully tested on real burst data from a Hewlett-Packard disk drive, but the results below more readily illustrate the benefits of the algorithm. The data shown below show the results of simulations comparing the Rectify and Integrate method of demodulation with two different implementations of the new algorithm. One uses only the fundamental harmonic of the burst signal and thus is called Sine Mixing. The second case uses the first, third, and fifth harmonics of the burst in the same proportions as they appear in the nominal noise-free burst. This will be called the Custom Harmonic method. A third method which is analogous to the Matched Filter approach uses all the harmonics in the nominal burst. As per the discussion in Section 2.1, we can show how this can sometimes yield undesirable results and thus may not be as good as the Custom Harmonic method.

As a measure of goodness we choose the nomalized standard deviation (σ_{nor}), *i.e.,* the standard deviation normalized by the true mean of amplitude which gives a number analogous to a signal to noise ratio. When we are generating a simulation, this true mean is the answer that one would get in the ideal, noise-free case. This is

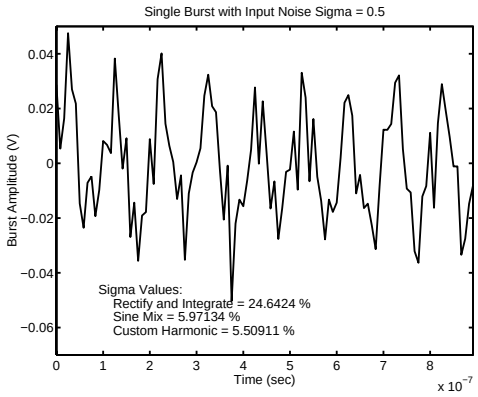

Figure 9: Single burst signal with additive noise. The standard deviation of the additive noise, (σ), is given by $\sigma = 0.5$. The units are normalized so that amplitude of the fundamental frequency of the burst is 1. The entire burst is then scaled by a factor of 0.02 to better match the amplitude of bursts measured in the lab.

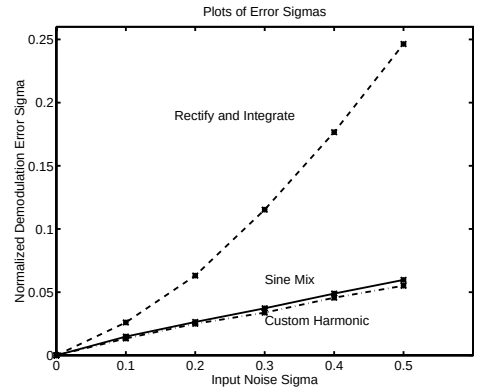

Figure 10: Comparison of standard deviations of Sine Mix and Custom Harmonic demodulation versus Rectify and Integrate demodulation schemes. The data was taken as the input noise on the burst was raised from $\sigma = 0$ to $\sigma = 0.5$ in the normalized units of the simulation.

computed as:

$$\sigma_{nor}(x) = \frac{E\{(x-\mu)^2\}^{\frac{1}{2}}}{\mu}. \qquad (9)$$

When a percentage is desired, the above number is multiplied by 100. In the case of measured bursts (where the true mean was not available), care was taken to compute the sample mean before passing the signal through any biasing operations (such as a rectifier).

3.1 Immunity to Broadband Noise

The new demodulator has greater immunity to broadband noise than the Rectify and Integrate method(Figure 10). (Note that the Rectify and Integrate method has better noise immunity than a standard Peak Detection scheme[6].) In current drives a typical input noise level would correspond to the abscissa value of 0.1 in Figure 10. At this level, the new demodulator has roughly a factor of 2 improvement in noise immunity. However, it is important to note that as the input noise level goes up, the advantage of the new demodulator increases dramatically.

3.2 Immunity to Signal Nonidealities

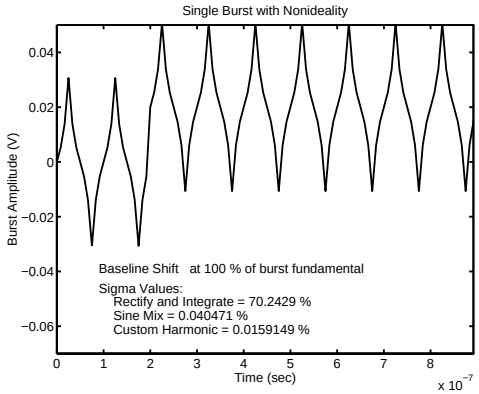

Figure 11: A noise-free burst with a baseline shift starting at the third dibit.

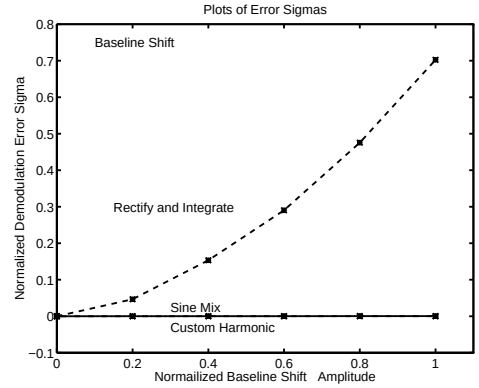

Figure 12: Comparison of standard deviations of Sine Mix and Custom Harmonic demodulation versus Rectify and Integrate demodulation schemes. The data was taken as the baseline shift starting at the third dibit was raised from 0 to 1.0 in the normalized units of the simulation.

This section addresses the addition of signal distortions or nonidealities. In order to have a common basis for comparison, several standards were maintained:

- A 9 dibit burst was always used to maintain consistency in the results and consistency with the disk drives from which measured data was obtained.
- No random noise was added in simulations where the nonidealities were being added.
- The nonidealities always were introduced at the start of the third dibit. This is for consistency and clarity of exposition.

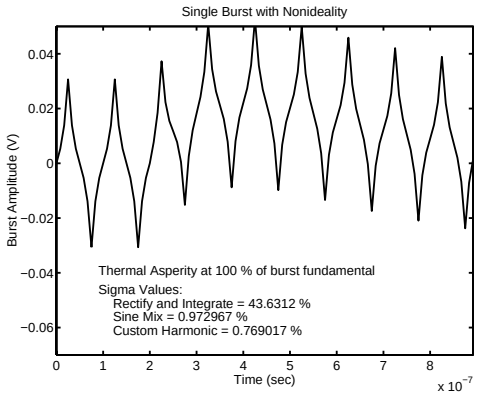

Figure 13: A noise-free burst with a thermal asperity starting at the third dibit.

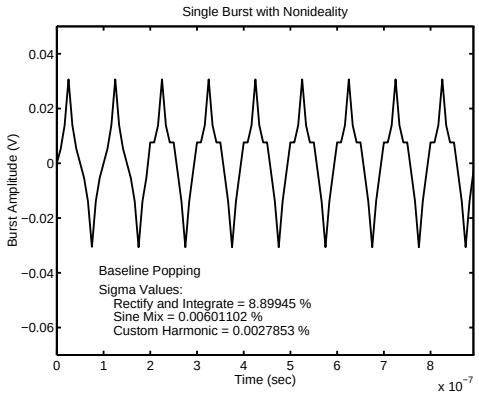

Figure 15: A noise-free burst with baseline popping starting at the third dibit.

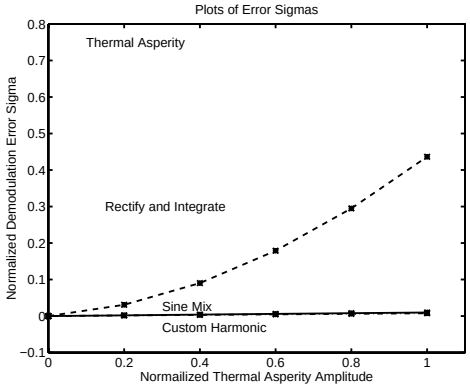

Figure 14: Comparison of standard deviations of Sine Mix and Custom Harmonic demodulation versus Rectify and Integrate demodulation schemes. The data was taken as the thermal asperity starting at the third dibit was raised from 0 to 1.0 in the normalized units of the simulation.

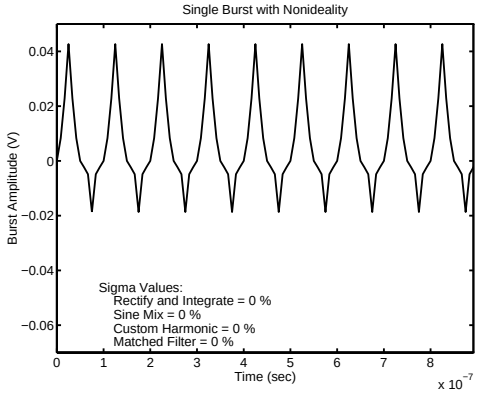

Figure 16: A noise-free burst with a nominal second harmonic distortion scaled to 0.3 of the fundamental frequency amplitude.

- The nonidealities were scaled relative to the amplitude of the fundamental frequency of the servo burst.

Baseline Shift is a sudden increase in the offset of the burst (Figure 11). It creates a large effect on the Rectify and Integrate demodulator, but virtually none on the new demodulator (Figure 12).

A **Thermal Asperity** causes a rapid increase and then gradual decrease in the response from the head (Figure 13). It creates a large effect on the Rectify and Integrate demodulator, but virtually none on the new demodulator (Figure 14).

With **Baseline Popping**, the nominal quiescent value of the a dibit pulse returns to a nonzero value (Figure 15). This causes some problems for the Rectify and Integrate detector, but none for the new demodulator. Unfortunately, this does not lend itself well to being plotted in the σ value plots, so only one example is given.

The **Second Harmonic Distortion** discussed in Section 2.1 is shown in Figure 16. It results in an asymmetric pulse shape. When the amount of second harmonic distortion deviates from the nominal level as shown in Figure 17, then both the Rectify and Integrate and Matched Filter methods exhibit dramatic error levels. This is due to the fact that since the Matched Filter demodulates frequencies that include the second harmonic distortion it demodulates the erroneous component as well, causing an error. Note that since neither the Sine Mix nor the Custom Harmonic schemes demodulate these frequencies, they are immune to any second harmonic distortion as shown in Figure 18.

4 Discussion

Note that in all cases, the Sine Mix demodulator and the Custom Harmonic demodulator provide dramatic improvement over standard Rectify and Integrate. The Custom Harmonic demodulator also always does better than the Sine Mix demodulator, but the difference is small. The choice of Custom Harmonic versus Sine Mix is really one of slightly improved noise immunity versus potentially greater complexity. Note, however, that two of the implementation methods simply store the mixing signal in ROM and thus there is no added complexity in implementing the Custom Harmonic version over the Sine Mix

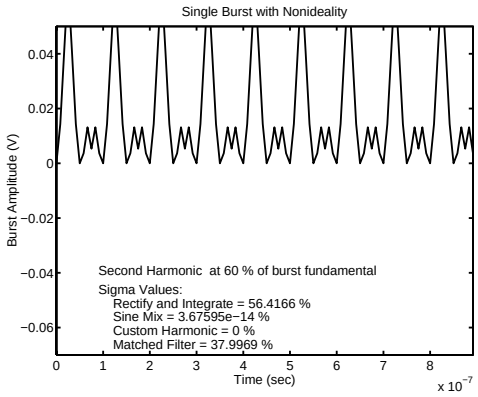

Figure 17: A noise-free burst with a nominal second harmonic distortion scaled to 0.3 of the fundamental frequency amplitude. An additional second harmonic distortion term of 0.6 of the fundamental frequency amplitude is added in.

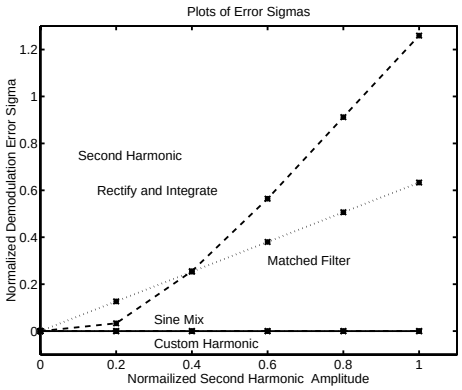

Figure 18: Comparison of standard deviations of Sine Mix, Custom Harmonic, and Matched Filter demodulation versus Rectify and Integrate demodulation schemes. To the noise-free burst withe the nominal second harmonic distortion scaled to 0.3 of the fundamental frequency amplitude was added additional second harmonic distortion terms scaled from 0 to 1.0 of the fundamental frequency amplitude is added in.

version. The improved noise immunity is essentially free.

Note that the Custom Harmonic method also gives more freedom to avoid such MR head phenomena as second harmonic distortion.

In summary, for the cost of some extra silicon in the servo demodulator, we can achieve dramatically improved immunity to both broadband noise and certain readback head phenomena which currently plague conventional servo demodulators. Furthermore, by removing the susceptibility to second harmonic distortion, the fact that the MR head produces an asymmetric pulse shape is irrelevant. The servo channel will only see the symmetric portion of the signal. This can save us the trouble of trying to remove this asymmetry in other ways (such as creating a dual stripe MR head or a dual stripe Giant Magneto-Resistive (GMR) or Colossal Magneto-Resistive (CMR) head).

Finally, while this paper has focused on applying the Customizable Coherent Demodulation Algorithm to disk drive servo loops, it should be usable in other real world systems.

Readers interested in a more detailed version of this paper are directed to the author's web page at http://www.hpl.hp.com/personal/Danny_Abramovitch/pubs/.

References

[1] D. Abramovitch, T. Hurst, and D. Henze, "An overview of the PES Pareto Method for decomposing baseline noise sources in hard disk position error signals," *IEEE Transactions on Magnetics*, pp. 17–23, January 1998.

[2] R. C. Blackham, J. A. Vasil, E. S. Atkinson, and R. W. Potter, "Measurement modes and digital demodulation for a low-frequency analyzer," *Hewlett-Packard Journal*, vol. 38, pp. 17–25, January 1987.

[3] D. Abramovitch, T. Hurst, and D. Henze, "The PES Pareto Method: Uncovering the strata of position error signals in disk drives," in *Proceedings of the 1997 American Control Conference*, (Albuquerque, NM), AACC, IEEE, June 1997.

[4] T. Hurst, D. Abramovitch, and D. Henze, "Measurements for the PES Pareto Method of identifying contributors to disk drive servo system errors," in *Proceedings of the 1997 American Control Conference*, (Albuquerque, NM), AACC, IEEE, June 1997.

[5] D. Abramovitch, T. Hurst, and D. Henze, "Decomposition of baseline noise sources in hard disk position error signals using the PES Pareto Method," in *Proceedings of the 1997 American Control Conference*, (Albuquerque, NM), AACC, IEEE, June 1997.

[6] Silicon Systems, *Integrated Circuits for Storage Products*, 1995.

[7] Z.-E. Boutaghou, D. H. Brown, K. J. Erickson, and R. Greenberg, "Digital servo signal demodulation method and apparatus utilizing a partial-response maximum-likelihood (prml) channel in a disk file," United States Patent 5,343,340, International Business Machines Corporation, Armonk, NY USA, Auguest 1994.

[8] H. Yada and T. Takeda, "A Coherent Maximum Likelihood Head Position Estimator for PERM Disk Drives," *IEEE Transactions on Magnetics*, May 1996.

[9] J. M. Mendel, *Lessons in Digital Estimation Theory*. Englewood Cliffs, NJ: Prentice-Hall, 1987.

[10] R. N. Bracewell, *The Fourier Transform and Its Applications*. New York: McGraw-Hill, 2 ed., 1978.